Search for Steady Emission of 10-TeV Gamma Rays from the Crab Nebula, Cygnus X-3, and Hercules X-1 Using the Tibet Air Shower Array

M. Amenomori,(1) Z. Cao,(2) L. K. Ding,(2) Z. Y. Feng,(3) K. Hibino,(4) N. Hotta,(5) Q. Huang,(3) A. X. Huo,(2) H. Y. Jia,(3) G. Z. Jiang,(3) S. Q. Jiao,(3) F. Kajino,(6) K. Kasahara,(7) Labaciren,(8) D. M. Mei,(8) L. Meng,(2) X. R. Meng,(8) Mimaciren,(8) K. Mizutani,(9) J. Mu,(10) H. Nanjo,(1) M. Nishizawa,(6) Nusang,(8) A. Oguro,(9) M. Ohnishi,(6) I. Ohta,(5) J. R. Ren,(2) To. Saito,(4) M. Sakata,(6) Z. Z. Shi,(2) M. Shibata,(11) T. Shirai,(7) H. Sugimoto,(12) X. X. Sun,(2) A. Tai,(10) K. Taira,(12) Y. H. Tan,(2) N. Tateyama,(7) S. Torii,(7) H. Wang,(2) C. Z. Wen,(3) Y. Yamamoto,(6) X. Y. Yao,(10) G. C. Yu,(3) P. Yuan,(2) T. Yuda,(4) J. G. Zeng,(3) C. S. Zhang,(2) H. M. Zhang,(2) L. Zhang,(10) Zhasang,(8) Zhaxiciren,(8) and W. D. Zhou(10)

(Tibet ASγ Collaboration)

(1)Department of Physics, Hirosaki University, Hirosaki, Japan
(2)Institute of High Energy Physics, Academia Sinica, Beijing, China
(3)Department of Physics, South West Jiaotong University, Chengdu, China
(4)Institute for Cosmic Ray Research, University of Tokyo, Tanashi, Japan
(5)Faculty of Education, Utsunomiya University, Utsunomiya, Japan
(6)Department of Physics, Konan University, Kobe, Japan
(7)Faculty of Engineering, Kanagawa University, Yokohama, Japan
(8)Department of Mathematics and Physics, Tibet University, Lhasa, China
(9)Department of Physics, Saitama University, Urawa, Japan
(10)Department of Physics, Yunnan University, Kunming, China
(11)Faculty of Education, Yokohama National University, Yokohama, Japan
(12)Shonan Institute of Technology, Fujisawa, Japan
(Received 11 June 1992)

The Tibet air shower array at an altitude of 4300 m (above sea level) has been in operation since January 1990. We have searched for continual emission of 10-TeV gamma rays from the Crab Nebula, Cygnus X-3, and Hercules X-1 during the period from June 1990 through January 1992. No dc excess is found from these three sources. Flux upper limits above 10 TeV are obtained to be 1.2×10^{-12} cm^{-2}s^{-1} for the Crab Nebula, 1.1×10^{-12} cm^{-2}s^{-1} for Cygnus X-3, and 0.58×10^{-12} cm^{-2}s^{-1} for Hercules X-1 at the 95% C.L. This is the first observation, with an air shower array, for these sources in the 10-TeV energy region.

PACS numbers: 98.70.Rz, 95.85.Qx, 97.80.Jp

Searches for very high energy (VHE) and ultrahigh energy (UHE) gamma-ray point sources have an important bearing on the origin of cosmic rays. Possible sources of this radiation are compact binaries, isolated pulsars, and supernova remnants. The most promising and well-known candidates in the northern sky are Cygnus X-3, Hercules X-1, and the Crab Nebula pulsar. The physical conditions inside these objects, with strong and rapidly rotating magnetic fields, high radiation densities, and large fluxes of relativistic particles, are particularly favorable for the generation of high energy gamma rays. However, there is, as yet, no universally accepted identification of the sources of UHE gamma rays, though many observations [1] have been made so far since the first report on the detection of UHE gamma rays from Cygnus X-3 by the Kiel group [2] in 1983. Recently the Whipple group [3] observed a steady emission of TeV gamma rays from the Crab Nebula with the high-resolution atmospheric Čerenkov camera and a signal was detected at the 20σ level which could be considered at a level for the detection to be credible. Although the flux is seemingly in favor of the synchrotron-self-Compton model reexamined by De Jager and Harding [4], confirmation requires further observations at higher energies, where experiments are beset with the difficulty of having to detect very low fluxes in the presence of considerable backgrounds of hadronic showers. Nevertheless, a search for gamma-ray signals is important and promising in the energy region around 10 TeV, and can be made with a high-resolution surface array. Observation at high altitude has advantages in observing air showers generated by very high energy gamma rays [5].

Here we report on the first results of the Tibet air shower experiment at Yangbajing, Tibet, in China [6,7]. It is located at Yangbajing International Cosmic Ray Observatory (90.53° E and 30.11° N) at an altitude of 4300 m (above sea level), corresponding to an atmospheric depth of 606 g/cm^2. The present array consists of 49 scintillation detectors of 0.5 m^2 each, which are deployed in a 7×7 matrix form with a separation of 15 m. Among them, 45 detectors (FT detectors) are equipped with fast response photomultipliers (PMT) with time jitter less than 0.55 ns to measure the arrival time of shower particles. A lead plate of 5 mm thickness is placed on the top of each detector to improve the fast timing data by converting gamma rays in air showers to electron pairs [8,9]. Another 16 scintillation detectors of 0.25 m^2 each surround the detector matrix to select showers whose cores fall in the array. The detector arrangement is schematically shown in Fig. 1.

The recording system is triggered by any fourfold coincidence of the FT detectors within a 300-ns time interval. The discrimination level of each detector for a trigger is set to the single-particle level, which results in a trigger rate of about 20 Hz. It takes about 5 ms to record one triggered shower, with the consequent dead time estimated to be about 10%. Data are stored on 8-mm videotape of 2.3 Gbyte capacity by using an EXB-8200 driver.

The Tibet air shower array has been in operation continuously since January 1990 and recorded about 6.3×10^8 shower events at a trigger rate of about 20 Hz during the period from 18 June 1990 through 14 January 1992. The effective running time for this period was 402.5 d.

Along with the experiment, Monte Carlo simulations have been done to examine the performance of the array as well as to compare with the experimental data, using the subroutine package GENAS developed by Kasahara and Torii [10]. Hadronic showers are generated by protons with a differential power-law spectrum of $E^{-\gamma}$, where γ changes from 2.73 to 3.00 at 2×10^{15} eV, while $\gamma = 2.0$ for gamma-induced showers. These showers are thrown uniformly over an area of radius 250 m for protons and 500 m for gamma rays, which are beyond where triggers are observed in our array. The observation conditions including the array structure and detector response are taken into account based on the experimental data.

For studies on cosmic-ray sources we first made a database by imposing the following conditions on the recorded events. (1) Each of any four FT detectors should detect a signal more than 1.25 particles. (2) Among the four detectors which record the highest particle densities, two or more should be in the inner 5×5 detectors. (3) The mean lateral spread of showers $\langle r \rangle$ should be less than 25 m, where $\langle r \rangle = \sum r_i \rho_i / \sum \rho_i$ and r_i is the distance of the ith detector from the estimated core and ρ_i its particle density. Events satisfying these conditions are called "contained" events: about 25% of the total recorded events. According to the simulation for gamma-induced showers, about 75% of the showers whose axes hit the 7×7 matrix region are rescued from elimination in this selection, while this fraction is slightly larger for proton-induced showers.

Figure 2 shows a $\sum \rho_{FT}$ distribution for the contained events, where ρ_{FT} denotes the number of shower particles per m^2 detected in each FT detector and the summation is taken over all FT detectors. The experimental result is almost consistent with the simulation for protons and a better fit in the small-size region will be obtained by taking the primary composition into account adequately. The mode value of the $\sum \rho_{FT}$ spectrum is about 26 m^{-2}, i.e., about thirteen particles in total. This corresponds to a primary energy of about 6 TeV for protons and about 8 TeV for gamma rays, respectively. Detection efficiencies of the contained events at 5, 10, and 50 TeV are estimated to be about 3%, 18%, and 78% for proton-induced showers, and 5%, 31%, and 80% for gamma-induced ones, respectively. Clearly, the Tibet air shower array is highly sensitive in the 10-TeV energy region (primarily because of the extreme altitude), and the observation can fill in the gap in energy between the TeV and PeV energy regions.

The ratio of signal from a point source to the isotropic background of hadronic showers is significantly increased by good angular resolution. For this, we studied core-finding and direction-determining techniques based on

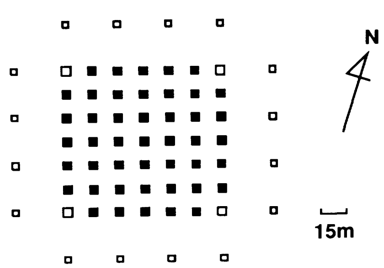

FIG. 1. Layout of the scintillation detectors in the Tibet air shower array. Solid squares stand for the FT detectors of 0.5 m^2 each.

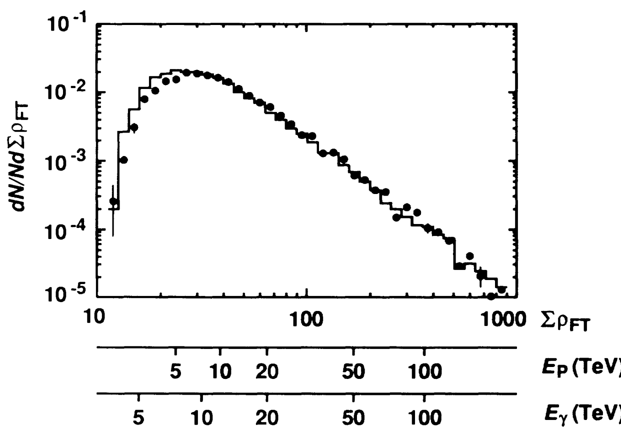

FIG. 2. Distribution of the sum of the number of shower particles per m^2 detected in each FT detector for the contained events. The experimental data are shown by the solid circles and the simulation result by the solid histogram. The energy scales, E_p and E_γ, show the mode primary energies for protons and gamma rays corresponding to the respective shower sizes.

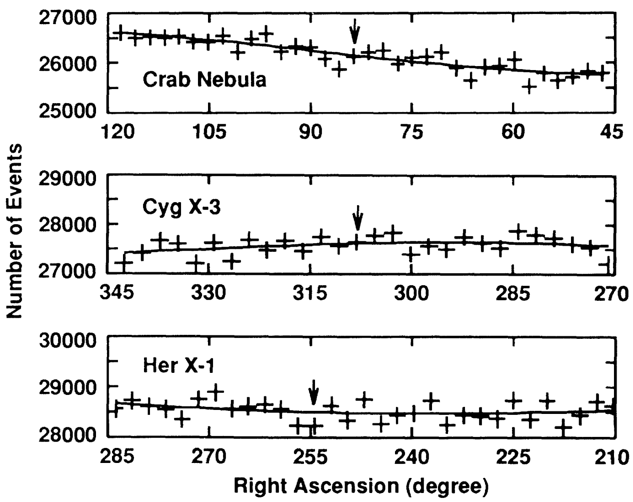

FIG. 3. Right-ascension scans of the events for the declination band centered on the Crab Nebula, Cygnus X-3, and Hercules X-1, respectively. The solid line for each source indicates the expected average level of cosmic-ray background.

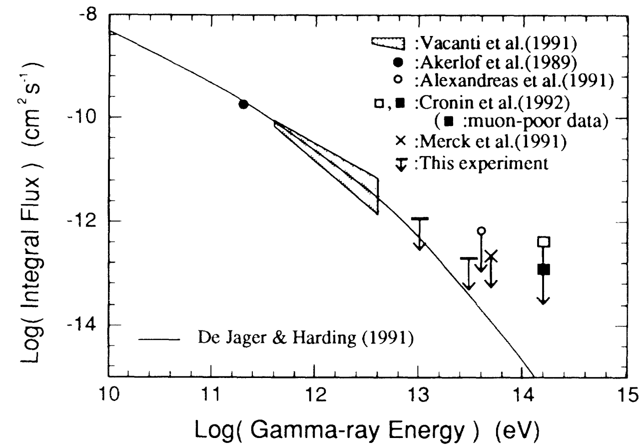

FIG. 4. A comparison of the experimental results for Crab fluxes and flux upper limits: Alexandreas *et al.* [13], Cronin *et al.* [14], Akerlof *et al.* [15], and Merck *et al.* [16]. The Whipple result [3] between 400 GeV and 4 TeV is shown by the shaded area. The solid line shows the calculation by De Jager and Harding [4].

the simulation results. The arrival direction of each shower is computed by determining the effective shower front from the timing signals in the FT detectors. The time structure of the shower front is approximated to be a cone surface. For showers in which 50% of all the contained events are included, the Monte Carlo simulations give an angular resolution of 1.0° for protons and 0.8° for gamma rays. The observation of the Moon's shadow by cosmic rays further confirmed that the angular resolution is 0.87° for all the events satisfying the selection criteria (1) and (2) [11].

Figure 3 shows the right-ascension scans for the Crab Nebula, Cygnus X-3, and Hercules X-1. The number of events coming from the region within a circle of apparent radius 1.0° is plotted as a function of right ascension at each declination of these sources. This window size is chosen to maximize the ratio $N_S/N_B^{1/2}$, where N_S is the number of signals and N_B the number of background events, and to contain about 50% of the signals from each source. The background contribution is estimated from events falling in the five windows adjacent to the source window at the same declination. The observed counts depend weakly on the right ascension as seen in Fig. 3, and almost the same behavior is observed for the three sources for all right ascensions, with a maximum variation of about 3.5%. This is mainly caused by the nonuniformity of data accumulation in sidereal time: long-term system stopping and diurnal variation of the trigger rate. We obtain 26 144 events for the Crab Nebula, 27 590 events for Cygnus X-3, and 28 493 events for Hercules X-1. The results of searching at the locations of the Crab Nebula, Cygnus X-3, and Hercules X-1 are excesses of -0.1σ, 0.3σ, and -1.7σ, respectively. We conclude that no evidence has been found for steady emission from those sources.

Upper limits on the excess number of events at the 95% confidence level are obtained: 348 for the Crab Nebula, 382 for Cygnus X-3, and 211 for Hercules X-1 assuming that the background and signal obey the Poisson distribution using the Protheroe procedure [12]. Then, flux upper limits for these sources are calculated using the Monte Carlo simulation. Showers from gamma rays are generated from a differential-power-law spectrum of the form $E^{-\gamma}$ with $E_{\min}=1$ TeV. The power index γ is assumed to be 2.0 both for Cygnus X-3 and Hercules X-1 and 2.4 for the Crab Nebula. Gamma rays are injected uniformly into the atmosphere along the constant declination for each source. Other conditions are the same as those mentioned above. The results are summarized in Table I.

Upper limit fluxes obtained above for the Crab Nebula are compared with other experiments in Fig. 4. The THEMISTOCLE group [17] also reported a positive effect for 3–10 TeV at the 4σ level using an eighteen-mirror array. Our results are near the flux levels extrapolated from the Whipple spectrum [3], $N(>E)=2.0\times10^{-11}(E/1\ \text{TeV})^{-1.4}\ \text{cm}^{-2}\text{s}^{-1}$, to our energy regions,

TABLE I. Flux upper limits above 10 and 30 TeV at the 95% confidence level for the Crab Nebula, Cygnus X-3, and Hercules X-1.

	$F(\geq 10$ TeV) (cm^{-2}s^{-1})	$F(\geq 30$ TeV) (cm^{-2}s^{-1})
Crab Nebula	1.2×10^{-12}	1.8×10^{-13}
Cygnus X-3	1.1×10^{-12}	1.4×10^{-13}
Hercules X-1	0.58×10^{-12}	1.7×10^{-13}

and are still compatible with the Compton-synchrotron model by De Jager and Harding [4]. This model needs abundant UHE electrons, possibly accelerated up to $\sim 3\times 10^{15}$ eV at the shock in the pulsar wind [18], and the smaller the magnetic field strength at the shock, the larger the UHE gamma-ray flux. Further observations at energies around 30 TeV can give a constraint to such a model. For Cygnus X-3, our limits are well below the levels obtained by extrapolation of the Kiel flux [2] back to the 10-TeV region, using an integral spectrum of E^{-1}, and our upper limit flux at 30 TeV is near or lower than the level of the CYGNUS experiment [13]. These clearly establish that Cygnus X-3 is no longer a steady source emitting VHE and UHE gamma rays at the Kiel flux level or has now fallen below the level of detectable emission. For Hercules X-1, extrapolating to higher energies shows that our results are at or near the levels reported by CYGNUS [13] and CASA [14], and place stringent flux upper limits at energies around 10–200 TeV.

In summary, we have searched for a steady emission of VHE or UHE gamma rays from the Crab Nebula, Cygnus X-3, and Hercules X-1 using the data obtained from June 1990 to January 1992. No dc excess is found from these three sources in this period, and stringent flux upper limits obtained in the 10-TeV energy region would place restrictions on the acceleration process of high-energy cosmic rays near discrete, point sources.

We are grateful to Professor J. Arafune of ICRR, University of Tokyo, and Professor S. X. Fan of IHEP, Academia Sinica, for their support and encouragement. We also wish to thank the staffs of the Geothermal Power Station at Yangbajing in Tibet for allowing us to use every facility necessary for carrying out the experiment. This work is supported in part by Grants-in-Aid for Scientific Research and also for International Scientific Research from the Ministry of Education, Science and Culture in Japan and the Committee of National Nature Science Foundation in China.

[1] T. C. Weekes, Space Sci. Rev. **59**, 315 (1992).
[2] M. Samorski and W. Stamm, Astrophys. J. **268**, L17 (1983).
[3] G. Vacanti *et al.*, Astrophys. J. **377**, 467 (1991).
[4] O. C. De Jager and A. K. Harding, in *Proceedings of the Twenty-Second International Cosmic Ray Conference, Dublin, Ireland, 1991* (The Dublin Institute for Advanced Studies, Dublin, Ireland, 1991), Vol. 1, p. 572.
[5] Y. Yamamoto *et al.*, in *Proceedings of the Workshop on Techniques in Ultra High Energy Gamma Ray Astronomy, La Jolla, 1985* (The University of Adelaide, Adelaide, 1985), p. 111.
[6] M. Amenomori *et al.*, *High Energy Gamma-Ray Astronomy,* AIP Conf. Proc. No. 220 (AIP, New York, 1991), p. 257.
[7] A. X. Huo *et al.*, in *Proceedings of the Twenty-First International Cosmic Ray Conference, Adelaide, Australia, 1990,* edited by J. Protheroe (Graphic Service, Northfield, South Australia, 1990), Vol. 2, p. 427.
[8] J. Linsley and A. A. Watson, J. Phys. G **14**, 645 (1988).
[9] M. Amenomori *et al.*, Nucl. Instrum. Methods Phys. Res., Sect. A **288**, 619 (1990).
[10] K. Kasahara and S. Torii, Comput. Phys. Commun. **64**, 109 (1991).
[11] M. Amenomori *et al.* (to be published).
[12] R. J. Protheroe, Astro. Expr. **1**, 33 (1984).
[13] D. E. Alexandreas *et al.*, Astrophys. J. **383**, 653 (1991).
[14] J. W. Cronin *et al.*, Phys. Rev. D **45**, 4385 (1992).
[15] C. W. Akerlof *et al.*, Nucl. Phys. B (Proc. Suppl.) **14A**, 237 (1990).
[16] M. Merck *et al.*, in *Proceedings of the Twenty-Second International Cosmic Ray Conference* (Ref. [4]), Vol. 1, p. 261.
[17] P. Baillon *et al.*, in *Proceedings of the Twenty-Second International Cosmic Ray Conference* (Ref. [4]), Vol. 1, p. 220. They have recently confirmed their results and derived an absolute flux [C. Ghesquiere (private communication)]. Their results are not inconsistent with ours.
[18] A. K. Harding and T. K. Gaisser, Astrophys. J. **358**, 561 (1990).

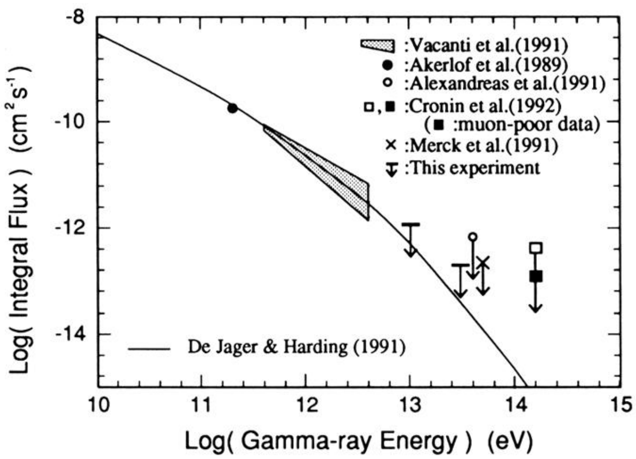

FIG. 4. A comparison of the experimental results for Crab fluxes and flux upper limits: Alexandreas *et al.* [13], Cronin *et al.* [14], Akerlof *et al.* [15], and Merck *et al.* [16]. The Whipple result [3] between 400 GeV and 4 TeV is shown by the shaded area. The solid line shows the calculation by De Jager and Harding [4].